Global and Planetary Change 162 (2018) 136–147

Contents lists available at ScienceDirect

Global and Planetary Change

journal homepage: www.elsevier.com/locate/gloplacha

Seasonal and elevational contrasts in temperature trends in Central Chile between 1979 and 2015

F. Burger[a,*], B. Brock[a], A. Montecinos[b]

[a] Department of Geography and Environmental Sciences, Northumbria University, Newcastle upon Tyne, UK
[b] Department of Geophysics, Water Research Center for Agriculture and Mining, Universidad de Concepcion, Chile

ARTICLE INFO

Editor: Dr. Fabienne Marret-Davies

Keywords:
Central Chile
Temperature trends
Climate change
Pacific influence
Seasonality

ABSTRACT

We analyze trends in temperature from 18 temperature stations and one upper air sounding site at 30°–35° S in central Chile between 1979–2015, to explore geographical and season temperature trends and their controls, using regional ocean-atmosphere indices. Significant warming trends are widespread at inland stations, while trends are non-significant or negative at coastal sites, as found in previous studies. However, ubiquitous warming across the region in the past 8 years, suggests the recent period of coastal cooling has ended. Significant warming trends are largely restricted to austral spring, summer and autumn seasons, with very few significant positive or negative trends in winter identified. Autumn warming is notably strong in the Andes, which, together with significant warming in spring, could help to explain the negative mass balance of snow and glaciers in the region. A strong Pacific maritime influence on regional temperature trends is inferred through correlation with the Interdecadal Pacific Oscillation (IPO) index and coastal sea surface temperature, but the strength of this influence rapidly diminishes inland, and the majority of valley, and all Andes, sites are independent of the IPO index. Instead, valley and Andes sites, and mid-troposphere temperature in the coastal radiosonde profile, show correlation with the autumn Antarctic Oscillation which, in its current positive phase, promotes subsidence and warming at the latitude of central Chile.

1. Introduction

Central Chile (30°–35° S) has a semi-arid Mediterranean climate, with the majority of precipitation falling in the winter half of year, which accumulates as snow in the Andes mountains above 2500 m (Falvey and Garreaud, 2007). Summers are characterized by low humidity, intense solar radiation and little rainfall at low elevations, although convective storms can produce significant precipitation in the high Andes (Pellicciotti et al., 2008; Viale and Garreaud, 2014). Climatic conditions show marked transitions with increasing distance from the coast, due to a decrease in the maritime influence from the Pacific Ocean, and the effects of topography (Garreaud, 2009). The combined influence of the cool Pacific Ocean and topographic barriers creates a persistent inversion layer in the lowest few hundred meters of the atmosphere (Aceituno et al., 1993; Falvey and Garreaud, 2009; Rutllant et al., 1995). Flows in lowland rivers, which are crucial for the region's economy, are heavily dependent on snow and glacier runoff in the summer and autumn months (Bravo et al., 2017).

Previous studies have identified spatial and temporal trends in temperature and precipitation in Chile over recent decades. Temperature rose significantly during the mid to late 20th century in coastal locations between 18 and 33°S (Rosenblüth et al., 1997), but then started to decrease, with a cooling trend up to $-0.20\,^{\circ}C\ decade^{-1}$ dominating over the past 20–30 years (Falvey and Garreaud, 2009). This trend reversal has been attributed to a shift to a negative phase of the Interdecadal Pacific Oscillation (IPO) (Vuille et al., 2015); itself inferred to be a consequence of global warming by a recent modeling study (Falvey and Garreaud, 2009). In contrast to the coastal cooling, inland Chile has experienced positive temperature trends in recent decades, at variable rates dependent on elevation (Falvey and Garreaud, 2009; Vuille et al., 2015), most likely due to anthropogenic climate warming (Vuille et al., 2015).

Annual temperature data may hide important contrasts in seasonal temperature trends. Cohen et al. (2012), for example, identified winter cooling over large parts of the extratropical northern hemisphere land surface since 1999, contrasting with warming trends in the other seasons. Vicente-Serrano et al. (2018) found a general warming trend in surface air temperature through Peru, identifying seasonal and spatial variations. Global and regional studies have recognized that seasonal changes in extremes of temperature often have high impacts on

* Corresponding author at: Department of Geography and Environmental Sciences, Northumbria University, NE1 8ST Newcastle upon Tyne, UK.
E-mail addresses: flavia.burger@northumbria.ac.uk (F. Burger), benjamin.brock@northumbria.ac.uk (B. Brock), amonteci@dgeo.udec.cl (A. Montecinos).

https://doi.org/10.1016/j.gloplacha.2018.01.005
Received 12 April 2017; Received in revised form 6 November 2017; Accepted 6 January 2018
Available online 17 January 2018

agriculture and hydrology (Alexander et al., 2006; Cortés et al., 2011; Menzel et al., 2006; Orlowsky and Seneviratne, 2012). In central Chile, glacier and snowpack mass balance and runoff may be sensitive to seasonal temperature changes. Hence, there is a need to conduct seasonally-disaggregated analyses to properly understand the impacts of climatic changes on the region's hydrology, which is heavily dependent on snow accumulation in the winter, and runoff from snow and ice melt during the arid summer months. Despite the potential importance of seasonal trends, to our knowledge, no seasonal analyses of recent climate change in central Chile have been conducted.

To address this shortcoming, the aim of this paper is to improve understanding of oceanic and topographic influences on spatial patterns of climatic change in central Chile, and in particular, how dominant modes of ocean–atmosphere circulation can result in contrasting seasonal temperature trends. We address this aim through (1) an analysis of seasonal and annual temperature trends in central Chile since 1979, in coastal, central valley and Andes geographical zones; and (2) evaluating the underlying drivers of climate trends through changes in atmospheric-oceanic circulation, quantified by the IPO and Antarctic Oscillation (AAO) indices, sea surface temperature, elevation and proximity to the Pacific coast. We focus on central Chile 30–35° S, as the most populous and economically important region of the country, where summer runoff from glacier and snow melt in the Andes is of vital importance to lowland flows of the major Aconcagua, Mapocho and Maipo river basins in the summer and autumn months. The period of analysis is from 1979 to 2015 due to the availability of extensive and reliable data for many ground stations in this period. We analyze data from 18 stations along a 200 km longitudinal corridor from coast to Andean cordillera centered on the heavily populated metropolitan region (30–35° S). This minimizes latitudinal climatic influences and better isolates the roles of Pacific Ocean–atmosphere circulation and anthropogenic warming, and their modulation by topography and proximity to ocean, in seasonal and spatial patterns of climate change. Station data are augmented with atmospheric soundings from the Quintero/Santo Domingo radiosonde sites. Two high elevation (> 2400 m above sea level, a.s.l.) stations enable us to identify temperature trends in the Andes compared to locations further to the west, to highlight important implications for the sustainability of snow and glacier water resources in the region.

2. Study area, data set and quality control

Two sources of temperature data are used in this study, covering the period between 1979 and 2015: observations at surface temperature stations (Table 1) and the radiosonde record from Quintero/Santo Domingo. Daily maximum and minimum surface temperature data were obtained from two National agencies: The Chilean water authority (Dirección General de Aguas, DGA) and the weather service (Dirección Meteorológica de Chile, DMC).

To analyze geographical patterns, stations within 18 km of the coast are referred to as “coastal”, locations above 2000 m a.s.l. are referred to as “Andes” while all other sites are referred to as “valley” locations.

2.1. Quality control

From the 102 stations available in the area between 30° and 35°S in Chile, only 18 stations have at least 34 years of data with < 15% of data missing in each year. Monthly means were calculated only for months with > 85% data per month. Data gaps were filled and data quality control applied using the following methods:

- Missing values. These were estimated from linear regression using reference series obtained from up to 5 neighboring stations significantly correlated with the candidate series. When no neighboring stations were available within 60 km of the candidate site, the station was discarded from the analysis.

Table 1
Details of temperature stations used in the analyses. Sites are shown in Fig. 1 with their respective ID number.

ID	Name	Latitude	Longitude	Elevation [m a.s.l.]
1	Rivadavia	−29.98	−70.56	820
2	La Ortiga	−30.19	−70.48	1560
3	La Laguna Embalse	−30.20	−70.04	3160
4	Paloma Embalse	−30.70	−71.04	320
5	Illapel	−31.65	−71.19	290
6	La Tranquilla	−31.90	−70.67	1000
7	Vilcuya	−32.86	−70.47	1100
8	Lliu-Lliu Embalse	−33.10	−71.21	260
9	Lago Peñuelas	−33.15	−71.56	360
10	Cerro Calán	−33.40	−70.54	848
11	Los Panguiles	−33.44	−71.03	190
12	Pirque	−33.67	−70.59	659
13	El Yeso Embalse	−33.68	−70.09	2475
14	La Serena	−29.92	−71.20	142
15	Quinta Normal Santiago	−33.45	−70.68	527
16	Curicó	−34.97	−71.22	225
17	Pudahuel Santiago	−33.39	−70.79	482
18	Tobalaba	−33.45	−70.55	650

- Outliers. Values outside the range of 3 standard deviations (std) around the climatological mean of the value for the day were defined as outliers, and were removed.
- Internal consistency. To ensure internal consistency in the temperature series, we tested that no maximum was lower than the minimum temperature of the previous day, (Hunziker et al., 2017), no inconsistency were found.
- Homogeneity. The standard normal homogeneity test (SNHT) developed by (Alexandersson, 1986; Alexandersson and Moberg, 1997) was applied to detect inhomogeneities, supplemented by visual inspection. As no metadata are available for these stations, the test was applied at 5% of significance. Detected inhomogeneities were treated using the same method as for missing values.

2.2. Trends calculation

Annual and seasonal trends in daily mean, maximum and minimum temperature were calculated using temperature anomalies, relative to the 1979–2010 mean temperature. The seasonal trends were calculated for temperature seasons: summer (December–February), autumn (March–May), winter (June–August), spring (September–November). The summer season was considered as commencing in December of the previous year, starting from December 1978.

As maximum and minimum temperature exhibit non-normal distributions, the non- parametric Mann-Kendall test (Kendall, 1938), was used to estimate the trends. To remove potential autocorrelation in the temperature time series, the methodology proposed by (Yue et al., 2002) was used. This approach has been successfully applied in previous hydro-meteorological studies, for example Cortés et al. (2011) and Hunziker et al. (2017). The procedure termed “Trend Free Pre-Whitening” (TFPW), involves the removal of the lag-1 autocorrelation for every time series showing significant autocorrelation. Finally, trends were tested, using the Kendall's tau based slope estimator (Sen, 1968), trends and correlations shown are considered statistically significant at the 5% level.

2.3. Quintero/Santo Domingo radiosonde record

Daily atmospheric soundings in central Chile are available since 1958, from the station located in Quintero (32°47′S, 71°33′W, 8 m a.s.l.), which was moved in 1999 to a new location at Santo Domingo (33°38′S, 71°18′W, 77 m a.s.l.). The soundings are launched twice a day (00 and 12 UTC), however, since soundings at 00 UTC are infrequent, only soundings at 12 UTC (08 local time) were used. Variables are

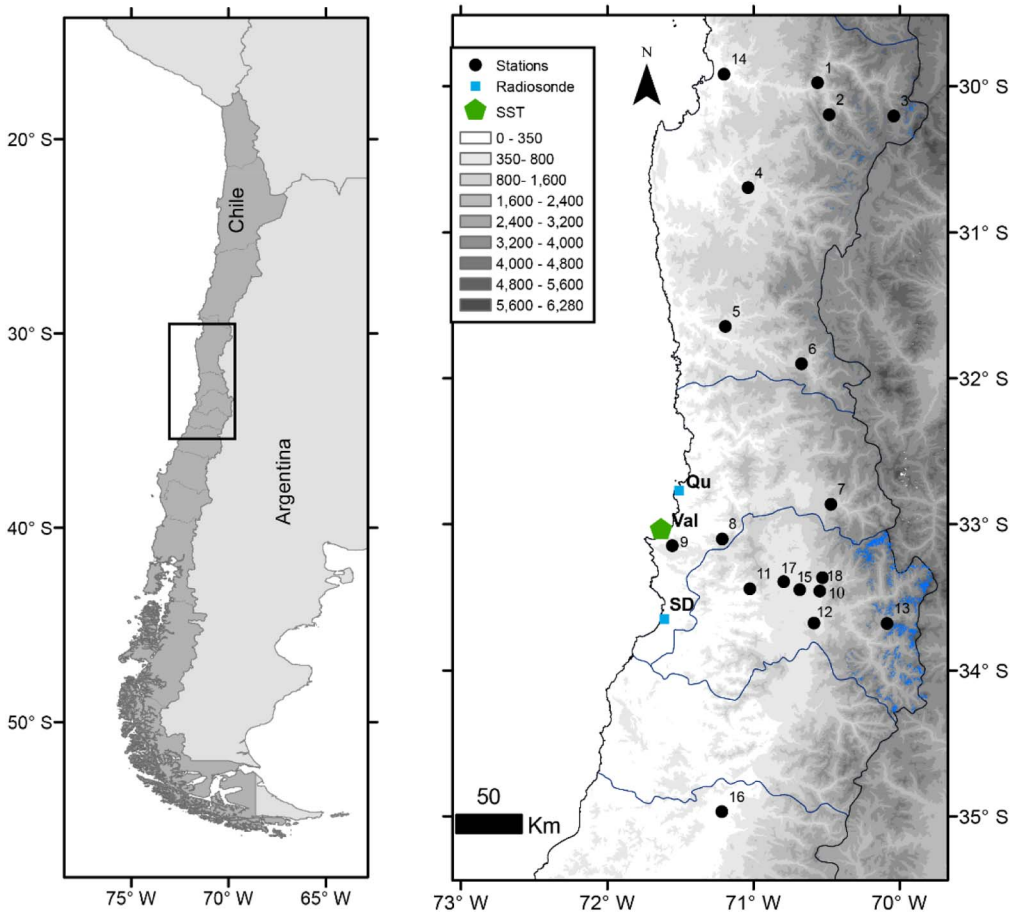

Fig. 1. The area of study in central Chile. Temperature stations are shown as black circles and blue squares mark radiosonde launch sites; glaciers area represented in blue shading. The background image is the SRTM DEM of February 2000. See Table 1 for full station names and site details. (For interpretation of the references to colour in this figure legend, the reader is referred to the web version of this article.)

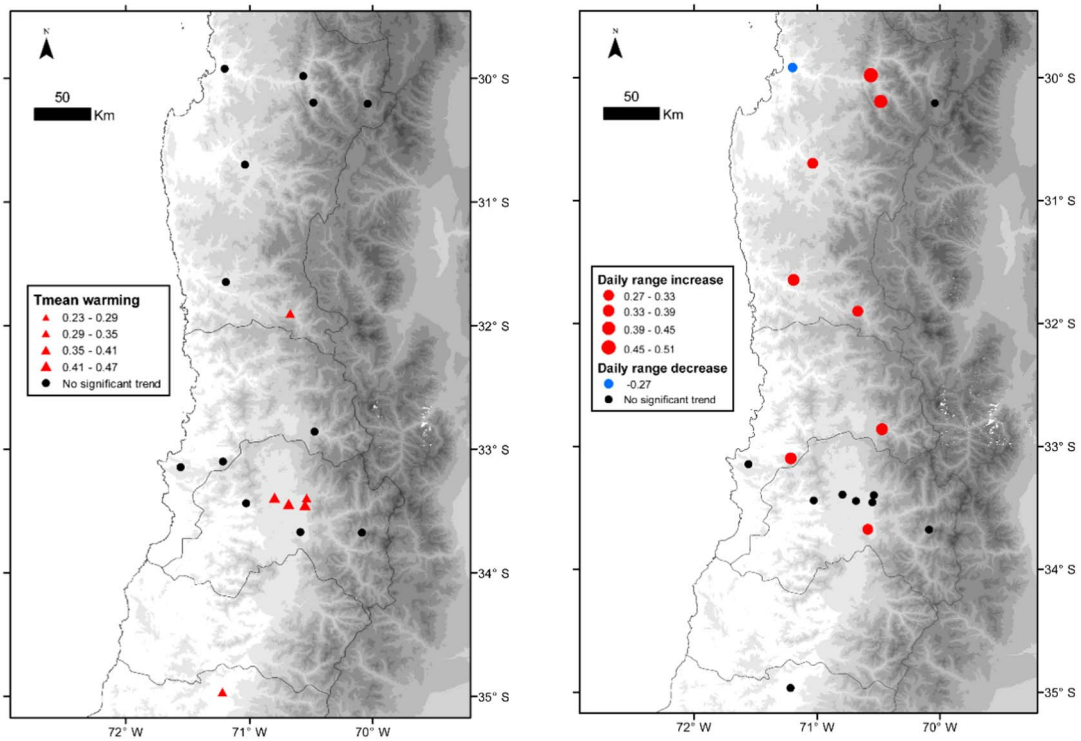

Fig. 2. Mean temperature (Tmean) trends (left panel) and daily temperature range (right panel) between 1979 and 2015. Significant warming trends are shown with red up pointing triangles and non-significant trends with black dots. (For interpretation of the references to colour in this figure legend, the reader is referred to the web version of this article.)

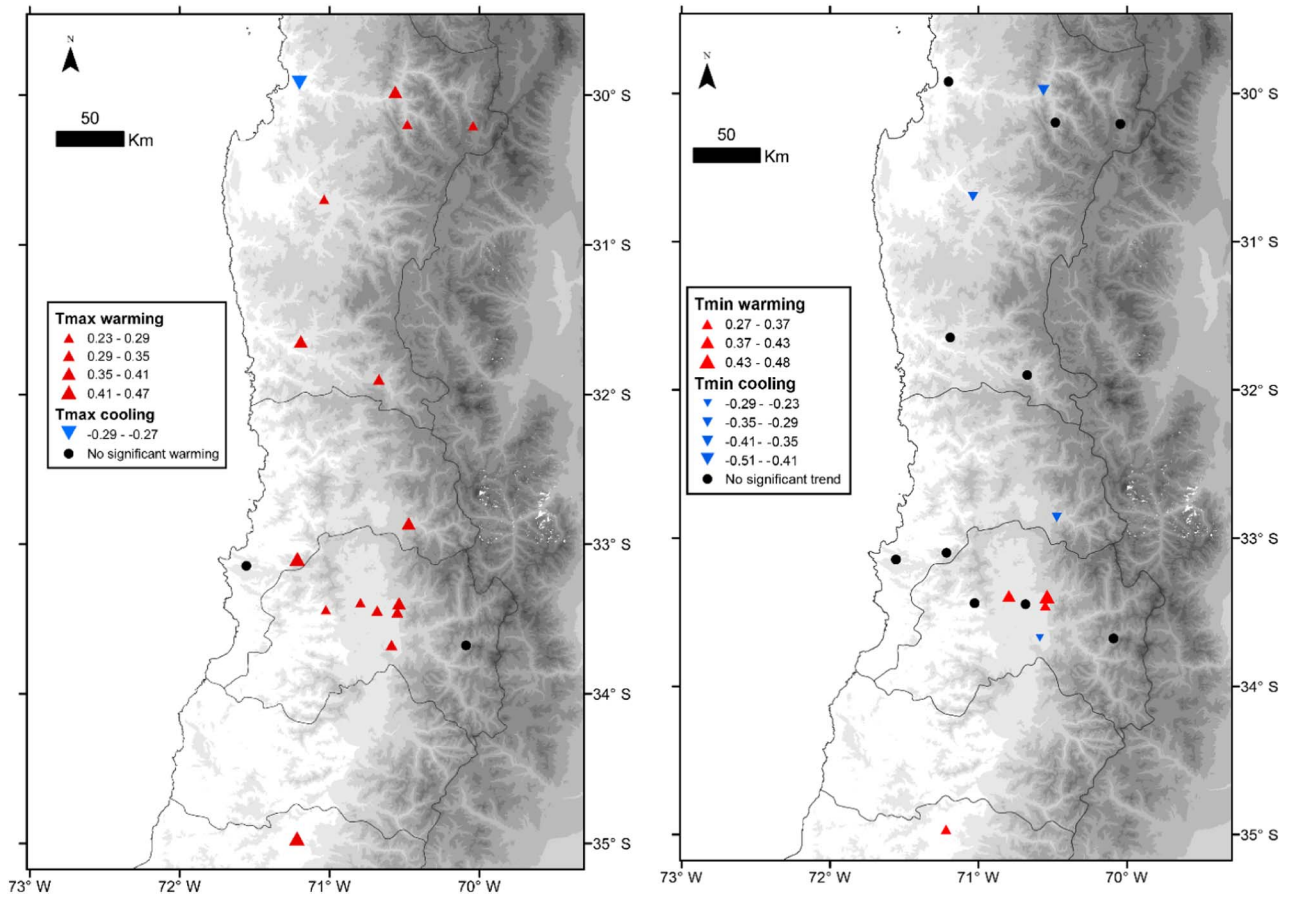

Fig. 3. Maximum temperature (left panel) and minimum temperature (right panel) trends between 1979 and 2015. Significant warming trends are shown with red up pointing triangles, while cooling trends are shown with blue down pointing triangles. Non-significant trends are identified with black dots. (For interpretation of the references to colour in this figure legend, the reader is referred to the web version of this article.)

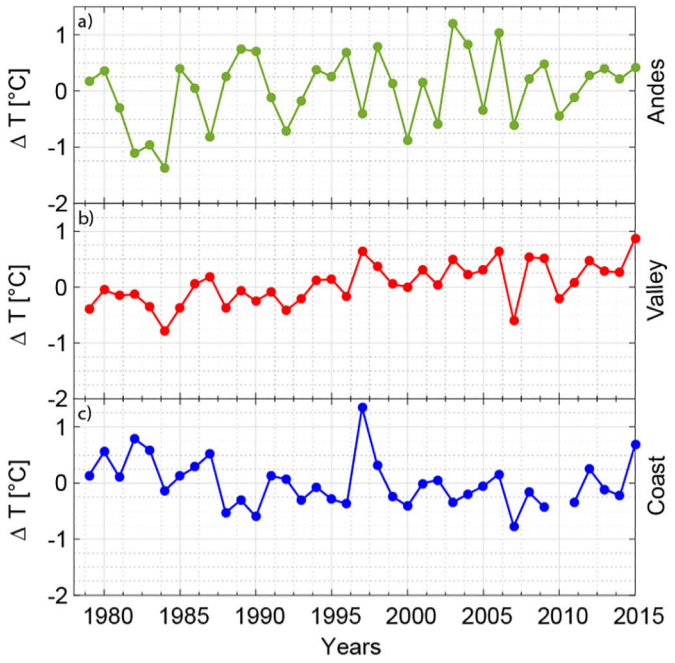

Fig. 4. Time series of annual temperature anomalies for geographical zones in central Chile, calculated with respect to the mean for the 1979 to 2010 reference period. (a) Andes, using Yeso Embalse (ID 13), (b) valley, using stations (ID 11-15-16-17-18), (c) coast, using La Serena Station (ID 10).

recorded at pressure levels, therefore, temperature data were hydrostatically interpolated onto a 100 m heights for use in this study. Owing to the shift of the launch site from Quintero to Santo Domingo in August 1999, temperature data after the move were adjusted using the difference between the mean of the 1979–1998 and 2000–2015 periods. The same methodology was applied by Rusticucci et al. (2014) to construct the winter 0 °C isotherm series with the same stations.

Finally, anomalies were calculated with respect to the 1979–2010 mean. The linear trend of annual mean temperature was calculated using least squares regression. The trend analysis was performed between elevations of 100 m and 6000 m covering the troposphere up to the elevation of the highest Andes summits in the region.

2.4. Analysis using regional ocean-atmosphere climatic indices

In order to evaluate potential drivers of observed temperature variability and trends in the study area, we analyzed the relationship with 2 regional ocean–atmosphere variability indices and sea surface temperature: (1) The Interannual Pacific Oscillation (IPO) index, which is a key index of multidecadal variability of the sea surface temperatures (SSTs) in the Pacific, covering different areas across the entire Pacific (Henley et al., 2015; Power et al., 1999; Salinger et al., 2001). The IPO series was provided by NOAA (http://www.esrl.noaa.gov/psd/data/timeseries/IPOTPI/). (2) The Antarctic Oscillation (AAO), also known as Southern Hemisphere Annular Mode (SAM), which is the lead index for the high latitude variability in the Southern Hemisphere, calculated as the first leading mode from the empirical orthogonal function (EOF) analysis of monthly mean height anomalies at 700 hPa (Gong and Wang, 1998); provided by NOAA (http://www.cpc.ncep.

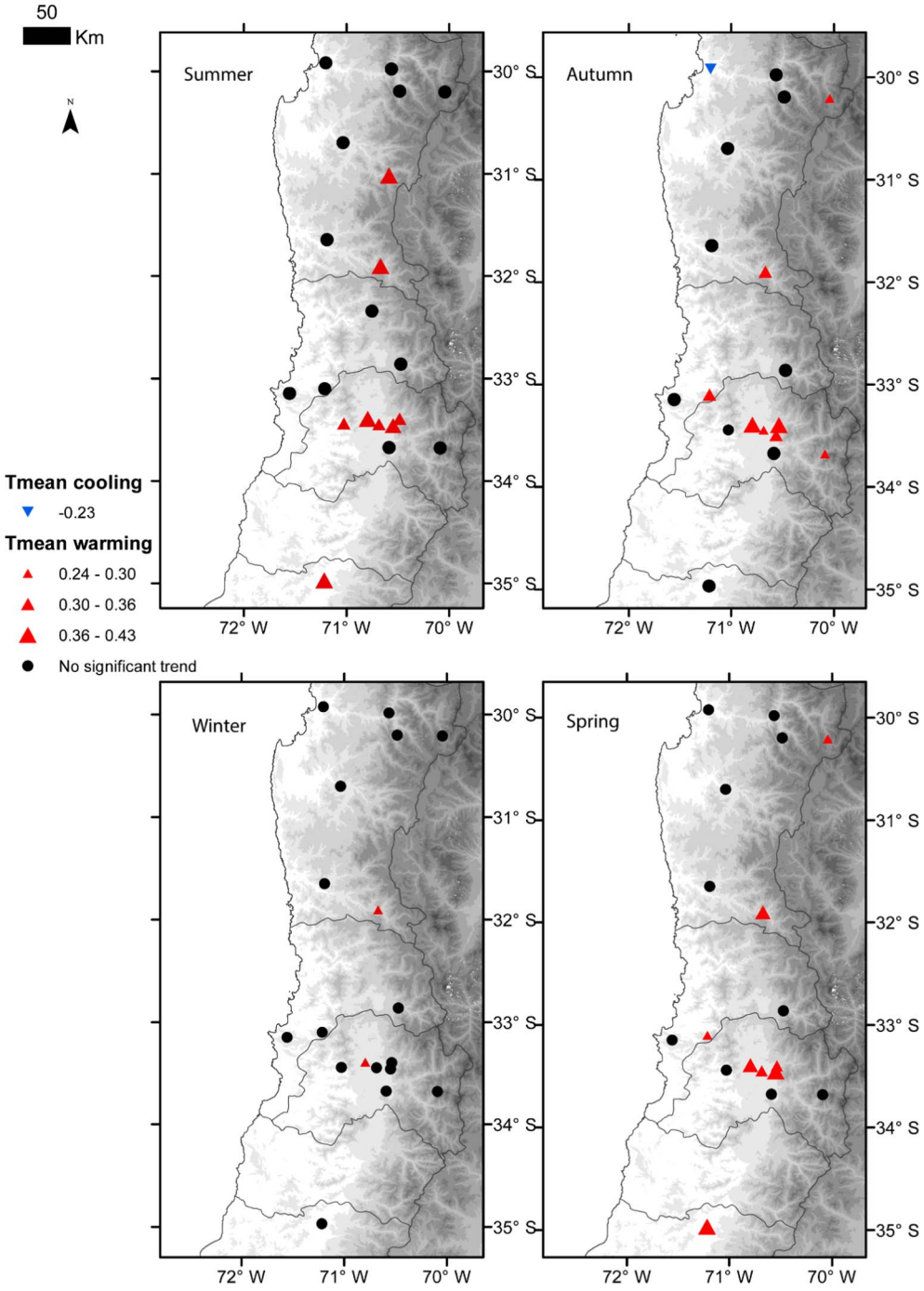

Fig. 5. Mean temperature trends per season between 1979 and 2015. Significant warming trends are shown with red up pointing triangles, and significant cooling trends are shown with blue down pointing triangles, while non-significant trends are identified with black dots. (For interpretation of the references to colour in this figure legend, the reader is referred to the web version of this article.)

noaa.gov/products/precip/CWlink/daily_ao_index/aao/aao.shtml). (3) Sea Surface temperature in Valparaiso (33.04°S, 71,61°W), was provided by the Chilean Navy Hydrographic and Oceanographic service (SHOA) http://www.shoa.cl/cendhoc/TSM_Datos/Valparaiso.txt.

3. Results

3.1. Temperature changes

3.1.1. Annual temperature trends in station data

Significant positive trends in mean annual temperature between 1979 and 2015 are identified at six valley sites, mainly in the metropolitan district and around Vilcuya (32°S) and at the most southerly site of Curicó (35°S), but trends are non-significant at all other sites (Fig. 2). Significant positive trends in annual maximum temperature (Fig. 3) are found at most of the sites except Yeso Embalse in the Andes and the coastal stations, with a significant maximum temperature cooling trend recorded on the coast at La Serena (around 30°S). In contrast, annual minimum temperature exhibits significant warming only in the Metropolitan Santiago area, while four valley sites at a range of latitudes show significant cooling trends, with non-significant trends in minimum temperature recorded at remaining sites (Fig. 3).

There is a general pattern of maximum temperatures rising faster than minimum temperatures at valley sites outside of Metropolitan Santiago, significantly increasing daily temperature amplitude. In contrast, on the coast, the decreasing trend of maximum temperature at La Serena has resulted in a decrease in daily temperature range.

Whereas significant warming trends between 1979–2015 are

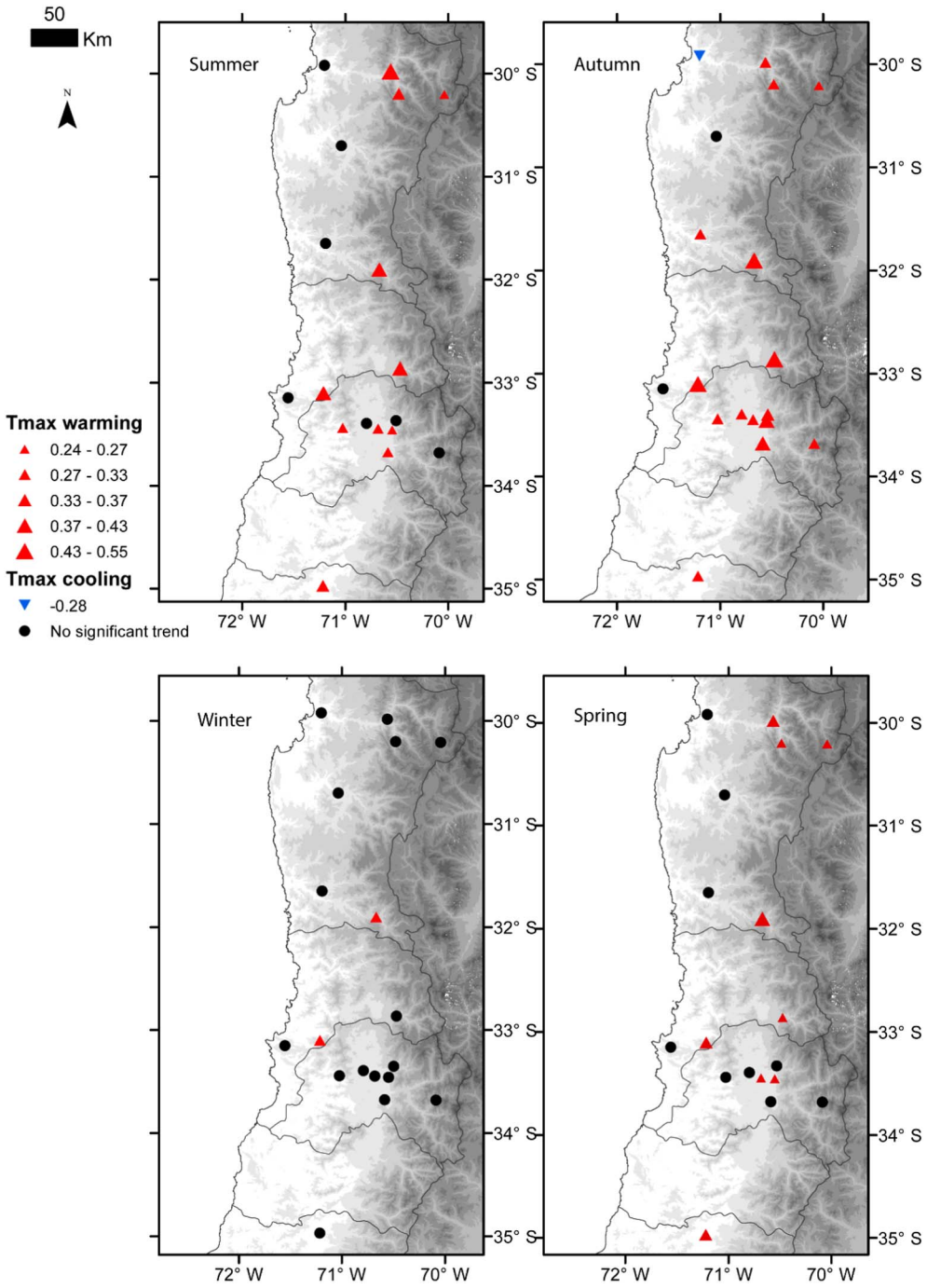

Fig. 6. Maximum temperature trends per season between 1979 and 2015. Significant warming trends are shown with red up pointing triangles, and significant cooling trends are shown with blue down pointing triangles. Non-significant trends are identified with black dots. (For interpretation of the references to colour in this figure legend, the reader is referred to the web version of this article.)

restricted to a few valley sites, all sites in the study region show significant warming between 2007 and 2015, including the coastal stations, at a mean rate of 1.1 °C decade^{-1} (Fig. 4). Indeed, 2015 was the warmest year on record in Santiago (Fig. 4) and globally (NOAA).

3.1.2. Seasonal temperature trends in station data

Significant warming trends are widespread at valley and Andes sites in the autumn, particularly for mean and maximum temperatures (Figs. 5 and 6). Significant warming trends in mean and maximum temperature are also identified at several valley and Andes sites in summer and spring. Warming trends in minimum temperature are restricted to a few valley, and one Andes, sites in spring, summer and autumn, with significant cooling trends in minimum temperature identified at some valley sites in spring, summer and autumn. In contrast to valley and Andes sites, which are dominated by warming trends, the coastal sites exhibit cooling, or non-significant temperature trends in all seasons (Figs. 5, 6 and 7). It is notable that the winter season exhibits few significant trends compared with other seasons, with only 2 sites (both valley) showing significant warming trends in mean and maximum temperature.

3.1.3. Annual and seasonal trends in radiosonde temperature

Annual temperature anomalies at El Yeso (2475 m a.s.l.) are significantly correlated with radiosonde annual temperature anomalies at 2400 m and 4000 m ($p < .05$; $r = 0.76$ and $r = 0.67$ respectively, Fig. 8a). The close agreement in the pattern of ground and atmosphere temperature anomalies throughout the time series lends confidence to the correction applied in this study (Section 2.4) to account for the change in radiosonde launch site in 1999. Interannual variations in the 0 °C (zero-degree) isotherm altitude (ZIA) are of the order of 10s–100s

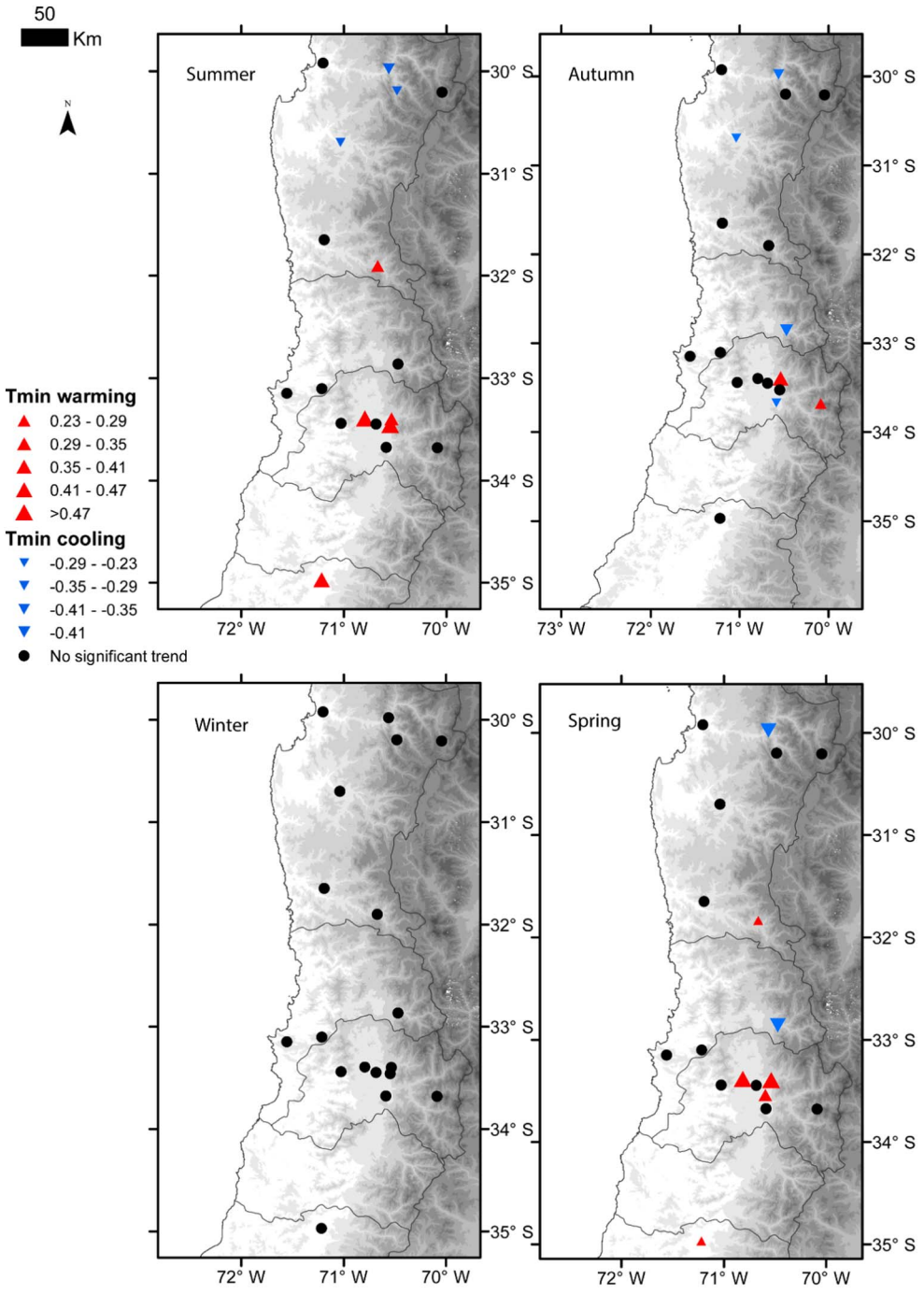

Fig. 7. Minimum temperature trends per season between 1979 and 2015. Significant warming trends are shown with red up pointing triangles, and cooling trends are shown with blue down pointing triangles non-significant trends are identified by black dots. (For interpretation of the references to colour in this figure legend, the reader is referred to the web version of this article.)

of m (Fig. 8b). Over the 1979–2015 period, there is a non-significant trend in annual or seasonal ZIA (not shown). Fig. 8b shows also the clear shift of mid 1970s, attributed of Pacific variability (Fig. 10a) and studied by Jacques-Coper and Garreaud (2014).

Over the 1979–2015 period annual mean tropospheric temperatures show a significant cooling trend near the surface but, with increasing elevation, there is a rapid transition to a non-significant annual trend at 400 m which remains non-significant, albeit with a positive sign, to the top of the studied profile at 6000 m (Fig. 9). However, this non-significant annual trend masks asymmetric seasonal trends, which suggest winter and spring cooling, and indicate significant warming in summer and autumn up to 4000 m elevation (Fig. 9b–e). There is significant cooling below 800 m in winter, but significant warming ($p < .1$) trends occur in summer between 300–2500 m, and in autumn between 400–4000 m, with a maximum of $+0.25\,^{\circ}C\ decade^{-1}$ at 3400 m.

3.2. Relationship of annual temperature variability to climate indices

At decadal timescales, following a marked shift to positive values in 1976, the IPO returned to negative values in the late 1990s and, although IPO values recovered slightly in the 2000s, they have remained at moderately low negative values in recent years (Fig. 10a). Over the same period, the AAO has increased from negative to positive values. The sea surface temperature in Valparaiso (Fig. 10b) shows high interannual variability, but broadly matches the pattern of the IPO, marked by the change to colder temperatures after 1999. However, in 2015 the sea surface temperature experienced a dramatic increase to positive anomalies.

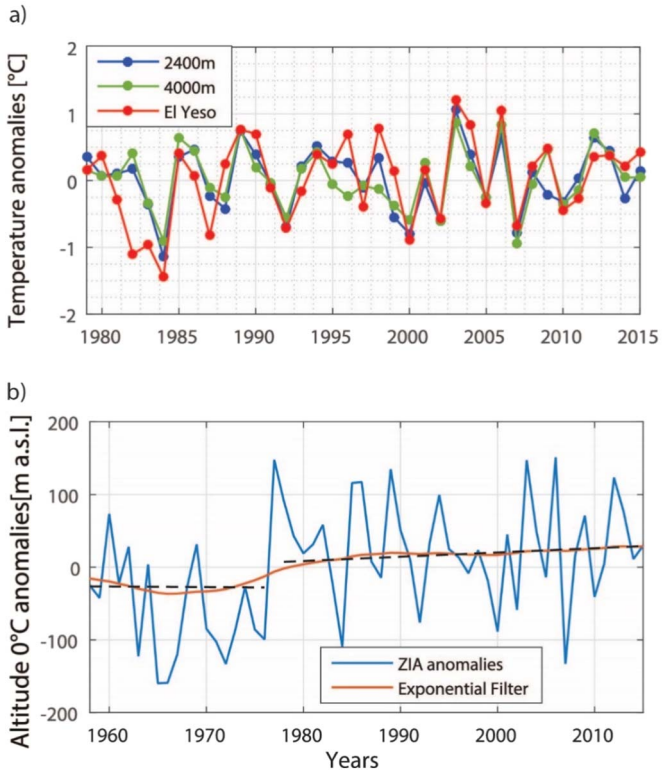

Fig. 8. a) Time series of temperature anomalies derived from radiosonde data at Quintero/Santo Domingo at 2400 m (blue line), and 4000 m (green line) and at El Yeso station at 2475 m, between 1979 and 2015, anomalies are relative to the 1979–2010 period. (b) Annual 0 °C isotherm altitudes (blue line) derived from the Quintero/Santo Domingo radiosonde for the period 1958–2015 and the same data with an exponential filter applied within that period (red line); dashed lines indicate the trends between1958 and 1976 and 1978 and 2015. (For interpretation of the references to colour in this figure legend, the reader is referred to the web version of this article.)

Mean annual temperatures at coastal stations show positive correlations with the IPO, while inland sites show non-significant correlations with the IPO, except at two western valley locations in the north of the region (Fig. 11). The influence of the AAO is most noticeable in autumn, where all valley and Andes stations east of the Santiago Metropolitan region, and Curicó to the south, show significant correlations in maximum temperature with the AAO index (Fig. 11b). This contrasts with non-significant correlations of maximum temperature and AAO in Santiago and western valley locations, and the significant negative correlation with the AAO at La Serena. Coastal tropospheric temperatures at 2400 and 4000 m a.s.l. also show positive correlations with AAO during autumn and in annual temperatures at 2400 m (Table 2). These results show a transition from the influence of the IPO near the coast, to the influence of the AAO at sites more distant from the coast in the valley and Andes, or above the inversion layer (coastal radiosonde at 2400 and 4000 m a.s.l.).

4. Discussion

4.1. Geographical and elevational variation in temperature trends

Mean annual temperature trends between 1979 and 2015 show a west-east transition from significant warming at inland sites, to non-significant trends or cooling at the coastal stations, most noticeably in maximum temperatures. This is consistent with earlier findings of (Falvey and Garreaud, 2009; Vuille et al., 2015). Coastal sites show significant positive correlations between mean annual temperature and the IPO. These results concur with Vuille et al. (2015), who found that coastal temperature series exhibit a strong congruence with the IPO and coastal sea surface temperature.

Further to these previous findings, we identify that the Pacific maritime influence weakens inland, and interannual and interdecadal temperature variations in the valley and Andes are independent of the IPO index and show instead a positive correlation with the AAO in autumn (Fig. 11). This suggests that the impact of cold phase of the IPO since the late 1990s has been restricted to the coastal zone directly influenced by the Pacific Ocean at elevations below the inversion layer (Aceituno et al., 1993; Rutllant et al., 1995). Hence, the slowing, or reversing, of warming trends over most of central Chile since 1979 did not occur at inland valley sites or Andes, which continued warming in this period. We identify no clear difference between annual warming trends in valley sites at around 500 m a.s.l. and Andes sites over 2400 m a.s.l. This contrasts with global trends which typically show warming rates increasing with elevation (Pepin et al., 2015).

The increase in daily temperature range at inland sites, resulting from maximum temperatures increasing faster than minimum temperatures, contrasts with some earlier work (Carrasco et al., 2005; Rosenblüth et al., 1997), who found that minimum temperature was rising quicker than the maximum temperature for the period 1960–1992 in central Chile. In contrast, La Serena on the coast shows convergence of maximum and minimum temperatures, resulting in a decreased daily temperature range.

The mechanism for these contrasting trends between coast and inland is unclear, but is likely to be related to the strength of Southeast Pacific Anticyclone (SEPA) since 1990 (Schneider et al., 2017; Valdés-Pineda et al., 2015a, 2015b), which promotes oceanic upwelling along the coast leading to reduced SST and coastal cooling (Kushnir et al., 2002; SenGupta and England, 2006) (Fig. 10b). Furthermore, strengthening of the SEPA in the negative IPO phase, enhances ocean upwelling off the coast of Chile (Garreaud and Falvey, 2009), stimulating offshore cooling due to cold air advection (Kushnir et al., 2002; SenGupta and England, 2006). An exception to this pattern is the Metropolitan Santiago region, which shows increasing trends of minimum temperature, which may well indicate a growing urban microclimate effect. The strength of the SEPA since 2000 has been linked to the recent expansion of the Hadley cell (Choi et al., 2014; Min and Son, 2013), itself a consequence of changes in greenhouse gases, aerosols and stratospheric ozone (Gillett et al., 2013; Min and Son, 2013).

The hiatus in warming since the end of the 1990s, identified at the same valley and coast sites by Falvey and Garreaud (2009), appears to have ended with all sites all showing strong warming in the past 8 years, consistent with the recent increase of the SST (Figs. 10b and 4). This return to a warming trend is consistent with an increase in the IPO away from strongly negative values in the early 2000s (Fig. 10a).

4.2. Seasonal contrasts in temperature trends

Seasonal warming is strongest and most widespread in autumn at valley and Andes stations, with maximum temperatures showing particularly strong trends (Fig. 6). Positive trends are also quite widespread in spring and summer.

The radiosonde profile also shows a significant negative trend in winter mean temperature below 300 m a.s.l., which contrasts with non-significant trends in station data at the same elevations, most likely due to boundary layer influences (Pepin and Seidel, 2005).

A probable explanation for the contrast between non-significant or cooling trends in winter and warming in other seasons is the decrease of the cyclonic activity in the storm track corridor under the influence of a strong SEPA since the late 1990s (Boisier et al., 2015; Schneider et al., 2017; Valdés-Pineda et al., 2015a, 2015b). A greater influence from the migratory anticyclone in central Chile produces more subsidence and increases the temperature in the valley and Andes due to adiabatic warming in spring, summer and autumn (Brock et al., 2012; Montecinos et al., 2017; Rutllant and Garreaud, 2004). Under the same scenario incursion of cooler, southerly air masses around the eastern side of the

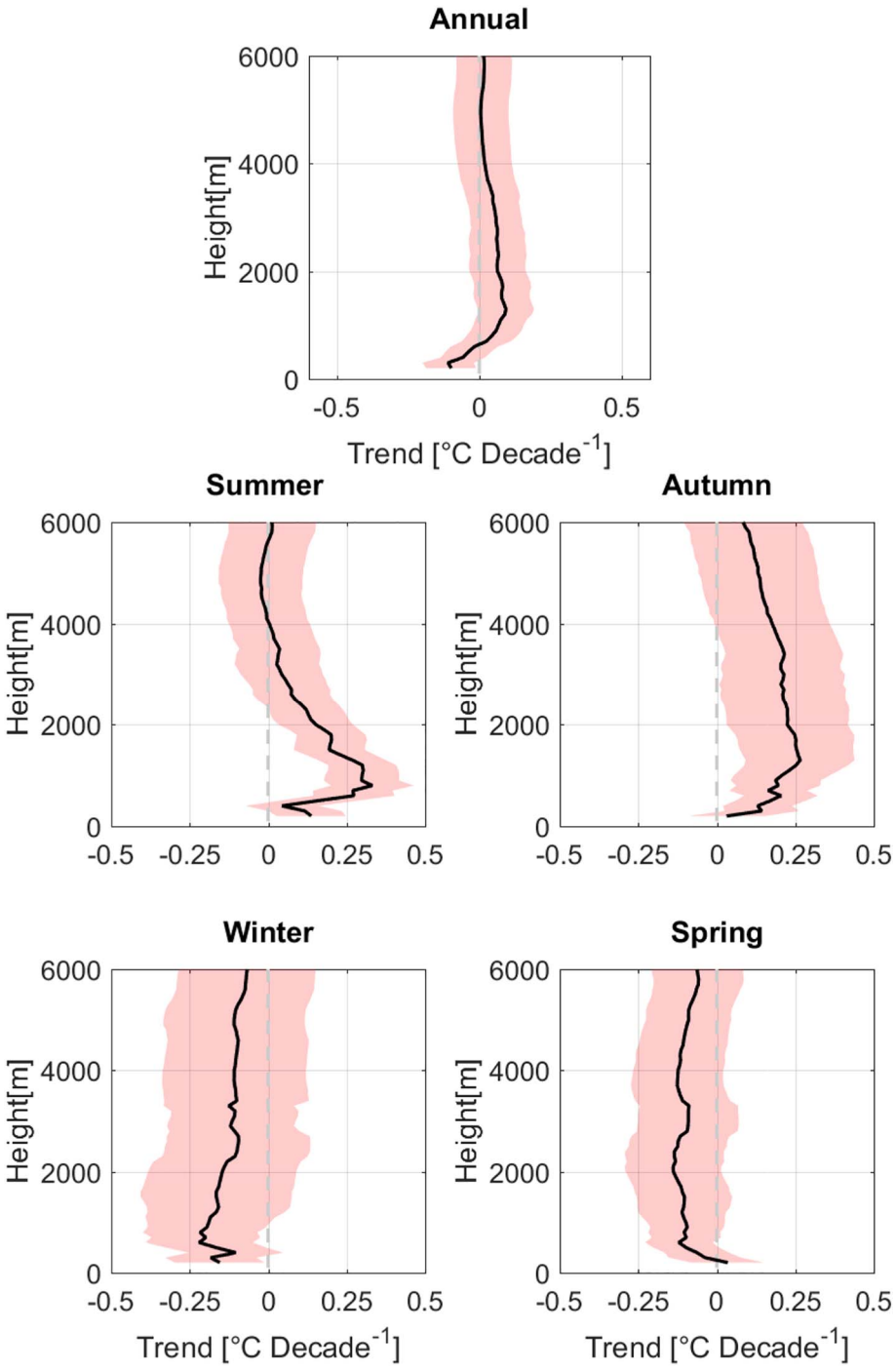

Fig. 9. Vertical profiles of temperature trends from the Quintero/Santo Domingo radiosonde for the period 1979–2015 for a) annual temperature and b–e) different seasons. The solid black lines represent the radiosonde trends at 100 m intervals and the shaded region indicates the 90% confidence interval.

SEPA, combined with lower cloud cover in winter, would enhance radiative cooling, particularly at night.

The strength of autumn warming inland is notable, particularly in the Andes (Figs. 5, 6 and 7) where a significant positive correlation between autumn temperature and the AAO index is identified. Hall and Visbeck (2002) have shown that during the positive phase of the AAO there is an increase of the westerlies around 60°S and subsidence throughout the mid and lower atmosphere north of 55° promoting adiabatic warming. It has been simulated that the decline of the aerosols and increase of greenhouse gases might be forcing the increase of the AAO and widening of the SEPA (Fyfe et al., 1999; Rotstayn, 2013), in turn affecting the temperatures in central Chile. A potential additional mechanism for late summer and autumn warming is due to positive feedbacks associated with reduced soil moisture and snow cover in the Andes leading to a lower evaporative energy flux and reduced local albedo (Rangwala and Miller, 2012).

The identified seasonal temperature trends in the Andes infer a strong negative impact on glacier mass balance, mainly through extending the ablation season length due to strong warming trends in the autumn, and also significant warming in spring. Recently, Masiokas et al. (2009, 2016) suggested that more research was needed to identify the climatic forcing behind glacier shrinkage in Central Andes of Chile and Argentina. The autumn seasonal trend, which shows a correlation with the positive phase of the AAO, helps to explain the dramatic regional glacier retreat recorded in recent decades despite moderate or weak mean annual and summer climatic warming signals (Bown et al., 2008; Bown and Rivera, 2007; Malmros et al., 2016; Masiokas et al., 2006, 2016; Rivera et al., 2002).

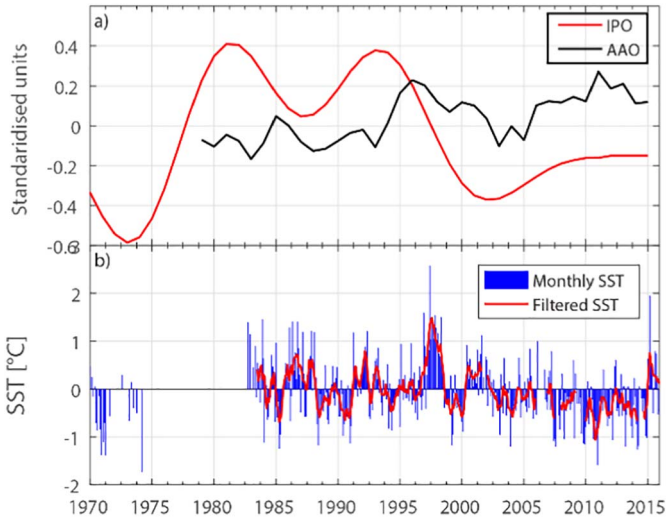

Fig. 10. (a) 11 years moving average filtered annual IPO (red line) and AAO (black line)) indices for the period 1970–2015. (b) Monthly Sea Surface temperature anomalies (SST) in Valparaiso 1970–2016 (blue bars) and a 5 month moving average filtered SST (red line). (For interpretation of the references to colour in this figure legend, the reader is referred to the web version of this article.)

5. Conclusions

In this study, we have investigated trends in temperature for the period 1979 to 2015 in the populous 30–35° S region of central Chile using data from 18 surface stations and one radiosonde site. The main aims were to examine variations in climate trends between: a) different seasons and b) different geographical zones, in order to improve understanding of regional climate change, its likely impacts, and its drivers, in particular the influence of regional Pacific Ocean-atmosphere circulation and Antarctic Oscillation. Our main conclusions are:

- As with previous studies, we identify a contrast between significant warming trends at inland sites and stationary or significant cooling trends at sites on the coast over recent decades. In central Chile, such stationarity and cooling is restricted to a narrow coastal strip, with a significant warming trend identified within 40 km of the coast.
- Notably, the regional cooling trend between 1979 and 2006 associated with the negative phase of the IPO identified by Garreaud and Falvey (2009) appears to have ended, with all sites showing warming to positive anomalies in the last 5 years, consistent with a marked rise in sea surface temperature at Valparaiso in 2015, and increase in the IPO index.
- Significant warming trends at inland sites are widespread in spring, summer and autumn, but there are few significant trends identified in winter. This finding, together with general divergence of maximum and minimum temperatures away from the coast (except under the influence of the urban microclimate of Metropolitan Santiago) might be explained by the strength of the South-East Pacific Anticyclone in the past 2 decades.
- Annual temperature variations are significantly positively correlated with the IPO index at coastal and two western valley locations, but correlation of annual temperature with the IPO index is non-significant at all other valley and Andes sites. This indicates a strong Pacific modulation of the anthropogenic warming signal on the coast which decreases in influence inland. Instead, the current positive phase of the AAO appears to influence temperatures in eastern valley and Andes sites, and at tropospheric elevations above the inversion layer, with widespread correlation of maximum temperature and AAO in the autumn.
- -The seasonal analysis conducted in this study has provided valuable insights into contrasting climatic trends in a relatively small

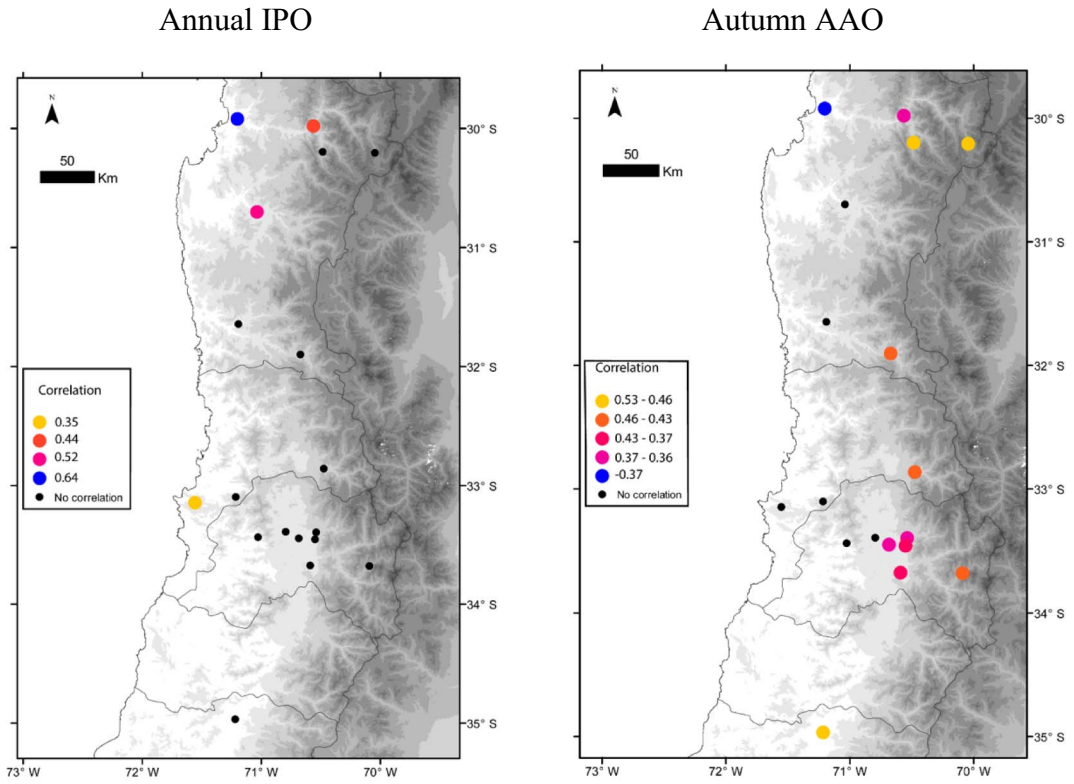

Fig. 11. Correlation between annual mean temperature and annual IPO (left panel) and correlation between maximum temperature in autumn and autumn AAO. Significance correlations (95% significant level) are shown as coloured circles. (For interpretation of the references to colour in this figure legend, the reader is referred to the web version of this article.)

Table 2
Seasonal and annual correlation between Radiosonde and seasonal values of AAO. ** indicates significant trends at the 95% confidence level, and * indicates significant trends at the 90% confidence level. AAO is the Antarctic Oscillation.

	Radiosonde 2400 m	Radiosonde 4000 m
	AAO	AAO
Summer	0.18	−0.07
Autumn	0.45**	0.34**
Winter	0.22	0.22
Spring	0.07	0.12
Annual	0.32*	0.28

geographical area. Further analyses of the seasonal changes of the AAO would help to understand further its influences on atmospheric circulation and seasonal temperature changes in central Chile, in particular in the high Andes.

Acknowledgments

Climatology data were provided by the Chilean Water Authority (Dirección General de Aguas, DGA), the weather service (Dirección Meteorológica de Chile, DMC). F.B. acknowledges Becas Chile scholarship from the Comisión Nacional de Investigación Científica y Tecnología de Chile, (CONICYT). A.M. was partially supported by CHRIAM/CONICYT/FONDAP-15130015. The IPO index was downloaded from (http://www.esrl.noaa.gov/psd/data/timeseries/IPOTPI/). The AAO index, was provided by NOAA http://www.cpc.ncep.noaa.gov/products/precip/CWlink/daily_ao_index/aao/aao.shtml

References

Aceituno, P., Fuenzalida, H., Rosenblüth, B., 1993. Climate along the extratropical west coast of South America. In: Earth Response to Global Change. Contrast Between North and South America. Academic Press, pp. 61–69.

Alexander, L.V., Zhang, X., Peterson, T.C., Caesar, J., Gleason, B., Klein Tank, A.M.G., Haylock, M., Collins, D., Trewin, B., Rahimzadeh, F., Tagipour, A., Rupa Kumar, K., Revadekar, J., Griffiths, G., Vincent, L., Stephenson, D.B., Burn, J., Aguilar, E., Brunet, M., Taylor, M., New, M., Zhai, P., Rusticucci, M., Vazquez-Aguirre, J.L., 2006. Global observed changes in daily climate extremes of temperature and precipitation. J. Geophys. Res. Atmos. 111, 1–22. http://dx.doi.org/10.1029/2005JD006290.

Alexandersson, H., 1986. A homogeneity test applied to precipitation data. J. Climatol. 6, 661–675.

Alexandersson, H., Moberg, A., 1997. Homogenization of Swedish Temperature Data. Part I: Homogeneity test for linear trends. Int. J. Climatol. 17, 25–34. http://dx.doi.org/10.1002/(SICI)1097-0088(199701)17:1<25::AID-JOC103>3.0.CO;2-J.

Boisier, J.P., Rondanelli, R., Garreaud, R.D., Muñoz, F., 2015. Anthropogenic and natural contributions to the Southeast Pacific precipitation decline and recent mega-drought in central Chile. Geophys. Res. Lett. 43, 413–421. http://dx.doi.org/10.1002/2015GL067265.

Bown, F., Rivera, A., 2007. Climate changes and recent glacier behaviour in the Chilean Lake District. Glob. Planet. Chang. 59, 79–86. http://dx.doi.org/10.1016/j.gloplacha.2006.11.015.

Bown, F., Rivera, A., Acuña, C., 2008. Recent glacier variations at the Aconcagua basin, central Chilean Andes. Ann. Glaciol. 48, 43–48. http://dx.doi.org/10.3189/172756408784700572.

Bravo, C., Loriaux, T., Rivera, A., Brock, B.W., 2017. Assessing glacier melt contribution to streamflow at Universidad Glacier, central Andes of Chile. Hydrol. Earth Syst. Sci. 21, 3249–3266. http://dx.doi.org/10.5194/hess-21-3249-2017.

Brock, B., Burger, F., Rivera, A., Montecinos, A., 2012. A fifty year record of winter glacier melt events in southern Chile, 38°–42°S. Environ. Res. Lett. 7, 45403. http://dx.doi.org/10.1088/1748-9326/7/4/045403.

Carrasco, J., Casassa, G., Quintana, J., 2005. Changes of the 0 °C isotherm and the equilibrium line altitude in central Chile during the last quarter of the 20th century. Hydrol. Sci. J. 50. http://dx.doi.org/10.1623/hysj.2005.50.6.933.

Choi, J., Son, S.-W., Lu, J., Min, S.-K., 2014. Further observational evidence of Hadley cell widening in the Southern Hemisphere. Geophys. Res. Lett. 41, 2590–2597. http://dx.doi.org/10.1002/2014GL059426.

Cohen, J.L., Furtado, J.C., Barlow, M., Alexeev, V.A., Cherry, J.E., 2012. Asymmetric seasonal temperature trends. Geophys. Res. Lett. 39, 1–7. http://dx.doi.org/10.1029/2011GL050582.

Cortés, G., Vargas, X., McPhee, J., 2011. Climatic sensitivity of streamflow timing in the extratropical western Andes Cordillera. J. Hydrol. 405, 93–109. http://dx.doi.org/10.1016/j.jhydrol.2011.05.013.

Falvey, M., Garreaud, R., 2007. Wintertime precipitation episodes in central Chile: associated meteorological conditions and orographic influences. J. Hydrometeorol. 8, 171–193. http://dx.doi.org/10.1175/JHM562.1.

Falvey, M., Garreaud, R.D., 2009. Regional cooling in a warming world: recent temperature trends in the southeast Pacific and along the west coast of subtropical South America (1979–2006). J. Geophys. Res. 114, 1–16. http://dx.doi.org/10.1029/2008JD010519.

Fyfe, J.C., Boer, G.J., Flato, G.M., 1999. The arctic and Antarctic oscillations and their projected changes under global warming. Geophys. Res. Lett. 26, 1601–1604. http://dx.doi.org/10.1029/1999GL900317.

Garreaud, R.D., 2009. The Andes climate and weather. Adv. Geosci. 7, 1–9.

Garreaud, R.D., Falvey, M., 2009. The coastal winds off western subtropical South America in future climate scenarios. Int. J. Climatol. 29, 543–554. http://dx.doi.org/10.1002/joc.1716.

Gillett, N.P., Fyfe, J.C., Parker, D.E., 2013. Attribution of observed sea level pressure trends to greenhouse gas, aerosol, and ozone changes. Geophys. Res. Lett. 40, 2302–2306. http://dx.doi.org/10.1002/grl.50500.

Gong, D., Wang, S., 1998. Definition of Antarctic oscillation index. Geophys. Res. Lett. 26, 459–462. http://dx.doi.org/10.1029/1999GL900003.

Hall, A., Visbeck, M., 2002. Synchronous variability in the Southern Hemisphere atmosphere, sea ice, and ocean resulting from the annular mode. J. Clim. 15, 3043–3057. http://dx.doi.org/10.1175/1520-0442(2004)017<2249:COSVIT>2.0.CO;2.

Henley, B.J., Gergis, J., Karoly, D.J., Power, S., Kennedy, J., Folland, C.K., 2015. A tripole index for the interdecadal Pacific Oscillation. Clim. Dyn. 45, 3077–3090. http://dx.doi.org/10.1007/s00382-015-2525-1.

Hunziker, S., Brönnimann, S., Calle, J.M., Moreno, I., Andrade, M., Ticona, L., Huerta, A., Lavado-Casimiro, W., 2017. Effects of undetected data quality issues on climatological analyses. Clim. Past Discuss. 2017, 1–31. http://dx.doi.org/10.5194/cp-2017-64.

Jacques-Coper, M., Garreaud, R.D., 2014. Characterization of the 1970s climate shift in South America. Int. J. Climatol. 35, 2164–2179. http://dx.doi.org/10.1002/joc.4120.

Kendall, M.G., 1938. A new measure of rank correlation. Biometrika 30, 81–93.

Kushnir, Y., Robinson, W.A., Bladé, I., Hall, N.M.J., Peng, S., Sutton, R., 2002. Atmospheric GCM response to extratropical SST anomalies: synthesis and evaluation. J. Clim. 15, 2233–2256. http://dx.doi.org/10.1175/1520-0442(2002)015<2233:AGRTES>2.0.CO;2.

Malmros, J.K., Mernild, S.H., Wilson, R., Yde, J.C., Fensholt, R., 2016. Glacier area changes in the central Chilean and Argentinean Andes 1955–2013. J. Glaciol. 62, 391–401. http://dx.doi.org/10.1017/jog.2016.43.

Masiokas, M.H., Villalba, R., Luckman, B., Le Quesne, C., Aravena, J.C., 2006. Snowpack variations in the central Andes of Argentina and Chile, 1951–2005: large-scale atmospheric influences and implications for water resources in the region. J. Clim. 19, 6334–6352.

Masiokas, M.H., Rivera, A., Espizua, L.E., Villalba, R., Delgado, S., Aravena, J.C., 2009. Glacier fluctuations in extratropical South America during the past 1000 years. Palaeogeogr. Palaeoclimatol. Palaeoecol. 281, 242–268. http://dx.doi.org/10.1016/j.palaeo.2009.08.006.

Masiokas, M.H., Christie, D.A., Le Quesne, C., Pitte, P., Ruiz, L., Villalba, R., Luckman, B.H., Berthier, E., Nussbaumer, S.U., González-Reyes, A., McPhee, J., Barcaza, G., 2016. Reconstructing glacier mass balances in the Central Andes of Chile and Argentina using local and regional hydro-climatic data. Cryosphere 10, 927–940. http://dx.doi.org/10.5194/tc-10-927-2016.

Menzel, A., Sparks, T.H., Estrella, N., Koch, E., Aaasa, A., Ahas, R., Alm-Kübler, K., Bissolli, P., Braslavska, O., Briede, A., Chmielewski, F.M., Crepinsek, Z., Curnel, Y., Dahl, A., Defila, C., Donnelly, A., Filella, Y., Jatczak, K., Måge, F., Mestre, A., Nordli, Ø., Peñuelas, J., Pirinen, P., Remisova, V., Scheifinger, H., Striz, M., Susnik, A., Van Vliet, A.J.H., Wielgolaski, F.E., Zach, S., Zust, A., 2006. European phenological response to climate change matches the warming pattern. Glob. Chang. Biol. 12, 1969–1976. http://dx.doi.org/10.1111/j.1365-2486.2006.01193.x.

Min, S.K., Son, S.W., 2013. Multimodel attribution of the Southern Hemisphere Hadley cell widening: major role of ozone depletion. J. Geophys. Res. Atmos. 118, 3007–3015. http://dx.doi.org/10.1002/jgrd.50232.

Montecinos, A., Muñoz, R., Oviedo, S., Martinez, A., 2017. Climatological characterization of Puelche winds in the extratropical western Andes Mountain using NCEP Climate Forecast System Reanalysis. J. Appl. Meteorol. Climatol. 56, 677–696. http://dx.doi.org/10.1175/JAMC-D-16-0289.1.

Orlowsky, B., Seneviratne, S.I., 2012. Global changes in extreme events: regional and seasonal dimension. Clim. Chang. 110, 669–696. http://dx.doi.org/10.1007/s10584-011-0122-9.

Pellicciotti, F., Helbing, J., Rivera, A., Favier, V., Corripio, J.G., Araos, J., Sicart, J.-E., Carenzo, M., 2008. A study of the energy balance and melt regime on Juncal Norte Glacier, semi-arid Andes of central Chile, using melt models of different complexity. Hydrol. Process. 22, 3980–3997. http://dx.doi.org/10.1002/hyp.

Pepin, N.C., Seidel, D.J., 2005. A global comparison of surface and free-air temperatures at high elevations. J. Geophys. Res. 110. http://dx.doi.org/10.1029/2004JD005047.

Pepin, N., Bradley, R.S., Diaz, H.F., Baraer, M., Caceres, E.B., Forsythe, N., Fowler, H., Greenwood, G., Hashmi, M.Z., Liu, X.D., Miller, J.R., Ning, L., Ohmura, A., Palazzi, E., Rangwala, I., Schöner, W., Severskiy, I., Shahgedanova, M., Wang, M.B., Williamson, S.N., Yang, D.Q., 2015. Elevation-dependent warming in mountain regions of the world. Nat. Clim. Chang. 5, 424–430. http://dx.doi.org/10.1038/nclimate2563.

Power, S., Casey, T., Folland, C., Colman, A., Mehta, V., 1999. Inter-decadal modulation of the impact of ENSO on Australia. Clim. Dyn. 15, 319–324. http://dx.doi.org/10.1007/s003820050284.

Rangwala, I., Miller, J.R., 2012. Climate change in mountains: a review of elevation-dependent warming and its possible causes. Clim. Chang. 114, 527–547. http://dx.doi.org/10.1007/s10584-012-0419-3.

Rivera, A., Acuña, C., Casassa, G., Bown, F., 2002. Use of remotely sensed and field data to estimate the contribution of Chilean glaciers to eustatic sea-level rise. Ann. Glaciol. 34, 367–372. http://dx.doi.org/10.3189/172756402781817734.

Rosenblüth, B., Fuenzalida, H.A., Aceituno, P., 1997. Recent temperature variations in south America. Int. J. Climatol. 17, 67–85.

Rotstayn, L.D., 2013. Projected effects of declining anthropogenic aerosols on the southern annular mode. Environ. Res. Lett. 8, 44028. http://dx.doi.org/10.1088/1748-9326/8/4/044028.

Rusticucci, M., Zazulie, N., Raga, G., 2014. Reginal winter climate of the southern central Andes: assessing the performance of ERA-Interium for climate studies. J. Geophys. Res. Atmos. 119, 8582–8588. http://dx.doi.org/10.1002/2013JD021167.

Rutllant, J.A., Garreaud, R.D., 2004. Episodes of strong flow down the western slope of the subtropical Andes. Mon. Weather Rev. 132, 611–622. http://dx.doi.org/10.1175/1520-0493(2004)132<0611:EOSFDT>2.0.CO;2.

Rutllant, J., Garreaud, R., Rutllant, José, Garreaud, Rene, 1995. Meteorological air pollution potential for Santiago, Chile: towards an objective episode forecasting. Environ. Monit. Assess. 34, 223–244.

Salinger, M.J., Renwick, J.A., Mullan, A.B., 2001. Interdecadal Pacific Oscillation and South Pacific climate. Int. J. Climatol. 21, 1705–1721. http://dx.doi.org/10.1002/joc.691.

Schneider, W., Donoso, D., Garcés-Vargas, J., Escribano, R., 2017. Water-column cooling and sea surface salinity increase in the upwelling region off central-south Chile driven by a poleward displacement of the South Pacific High. Prog. Oceanogr. 151, 38–48. http://dx.doi.org/10.1016/j.pocean.2016.11.004.

Sen, P., 1968. Estimates of the regression coefficient based on Kendall's tau. J. Am. Stat. Assoc. 63, 1379–1389.

SenGupta, A., England, M.H., 2006. Coupled ocean–atmosphere–ice response to variations in the southern annular mode. J. Clim. 19, 4457–4486. http://dx.doi.org/10.1175/JCLI3843.1.

Valdés-Pineda, R., Pizarro, R., Valdés, J.B., Carrasco, J.F., García-Chevesich, P., Olivares, C., 2015a. Spatio-temporal trends of precipitation, its aggressiveness and concentration, along the Pacific coast of South America (36°–49°S). Hydrol. Sci. J. 61, 2110–2132. http://dx.doi.org/10.1080/02626667.2015.1085989.

Valdés-Pineda, R., Valdés, J.B., Diaz, H.F., Pizarro-Tapia, R., 2015b. Analysis of spatio-temporal changes in annual and seasonal precipitation variability in South America-Chile and related ocean-atmosphere circulation patterns. Int. J. Climatol. 36, 2979–3001. http://dx.doi.org/10.1002/joc.4532.

Viale, M., Garreaud, R., 2014. Summer precipitation events over the western slope of the subtropical Andes. Mon. Weather Rev. 142, 1074–1092. http://dx.doi.org/10.1175/MWR-D-13-00259.1.

Vicente-Serrano, S.M., López-Moreno, J.I., Correa, K., Avalos, G., Bazo, J., Azorin-Molina, C., Domínguez-Castro, F., El Kenawy, A., Gimeno, L., Nieto, R., 2018. Recent changes in monthly surface air temperature over Peru, 1964–2014. Int. J. Climatol. 38, 283–306. http://dx.doi.org/10.1002/joc.5176.

Vuille, M., Franquist, E., Garreaud, R., Sven, W., Casimiro, L., Cáceres, B., 2015. Impact of the global warming hiatus on Andean temperature. J. Geophys. Res. Atmos. 120, 3745–3757. http://dx.doi.org/10.1002/2015JD023126.

Yue, S., Pilon, P., Phinney, B., Cavadias, G., 2002. The influence of autocorrelation on the ability to detect trend in hydrological series. Hydrol. Process. 16, 1807–1829. http://dx.doi.org/10.1002/hyp.1095.